Science Advances
AAAS

advances.sciencemag.org/cgi/content/full/6/51/eabd1580/DC1

Supplementary Materials for

Chemical anti-corrosion strategy for stable inverted perovskite solar cells

Xiaodong Li, Sheng Fu, Wenxiao Zhang, Shanzhe Ke, Weijie Song, Junfeng Fang*

*Corresponding author. Email: jffang@phy.ecnu.edu.cn

Published 16 December 2020, *Sci. Adv.* **6**, eabd1580 (2020)
DOI: 10.1126/sciadv.abd1580

This PDF file includes:

Figs. S1 to S13
Table S1

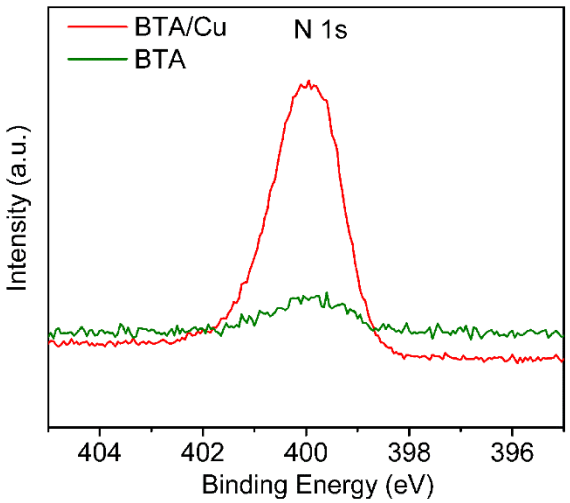

Fig. S1. XPS of N1s in pure BTA and Cu film deposited with BTA (BTA/Cu).

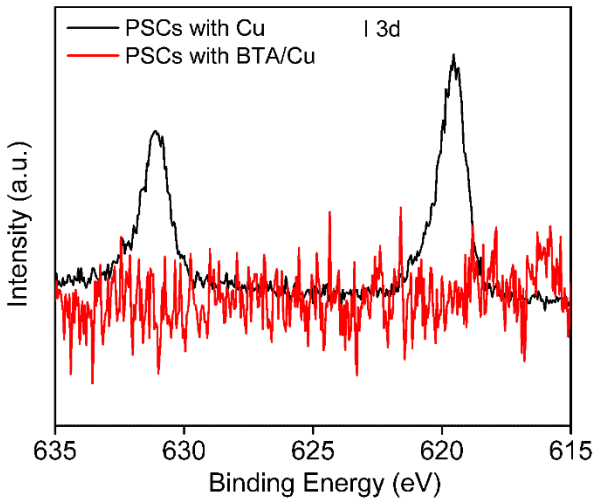

Fig. S2. XPS of I 3d on Cu electrode in PSCs after aging at 85 ^{o}C.

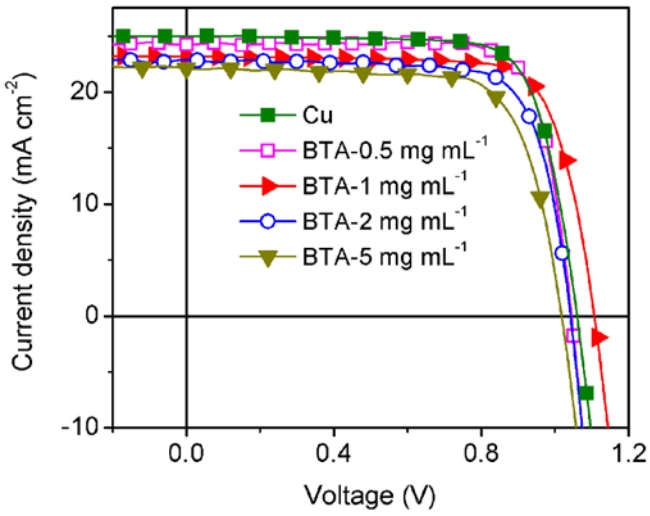

Fig. S3. *J-V* curves of BTA/Cu-based PSCs with different concentration of BTA.

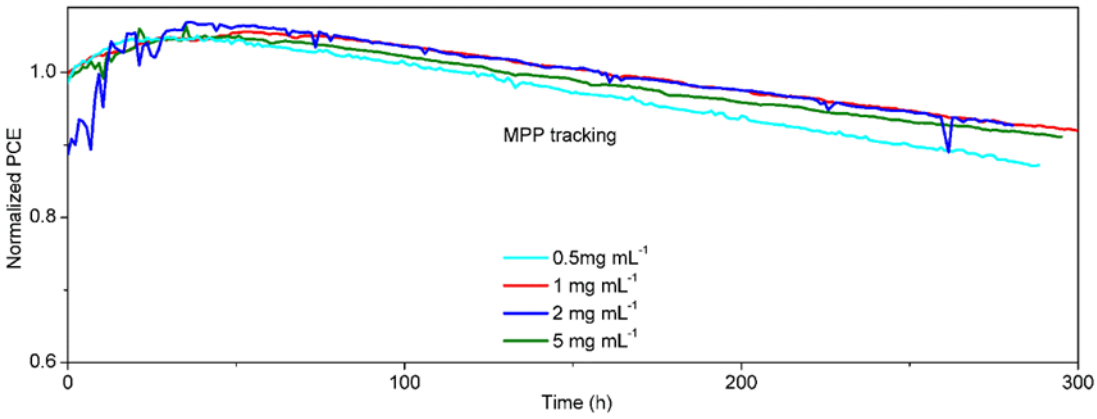

Fig. S4. Devices stability of Cu/BTA based PSCs with different concentration of BTA under continuous MPP tracking.

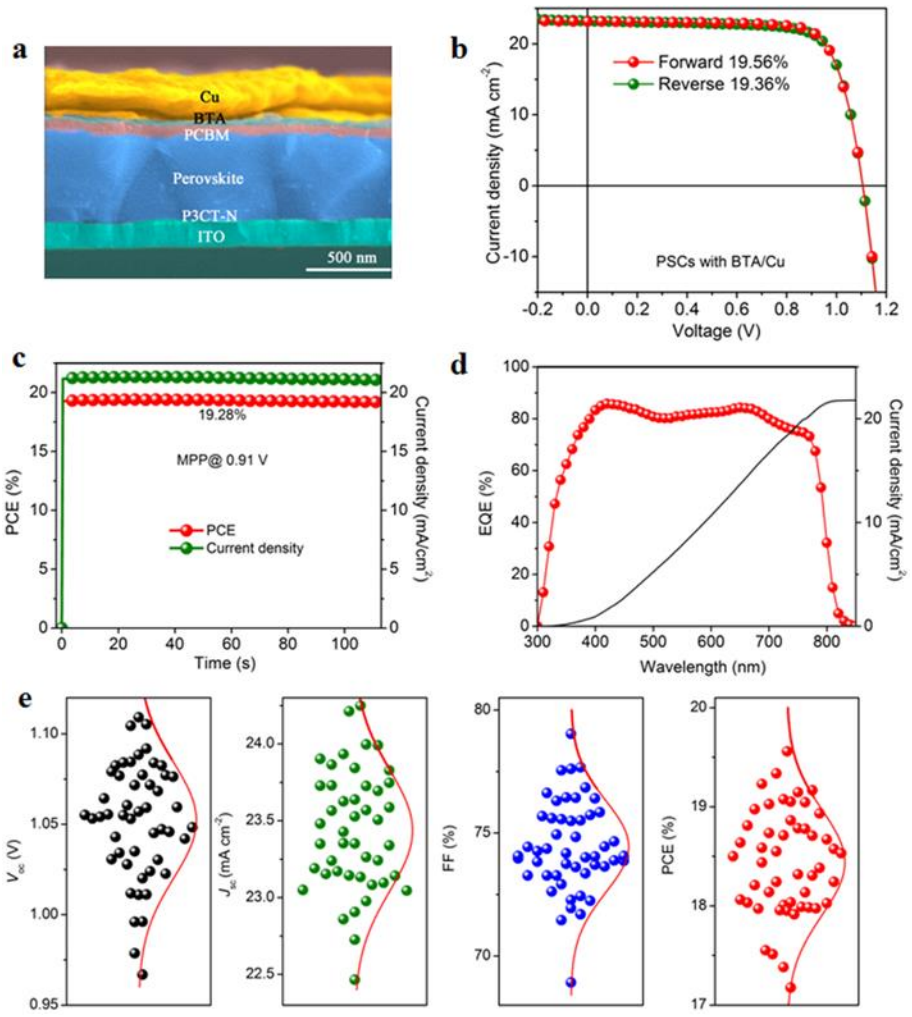

Fig. S5. Device performance of PSCs with BTA/Cu (BTA of 1mg mL^{-1}). (a) Cross-sectional SEM images of PSCs with BTA/Cu electrode. (b) J-V curves, (c) Stabilized MPP output, (d) EQE.

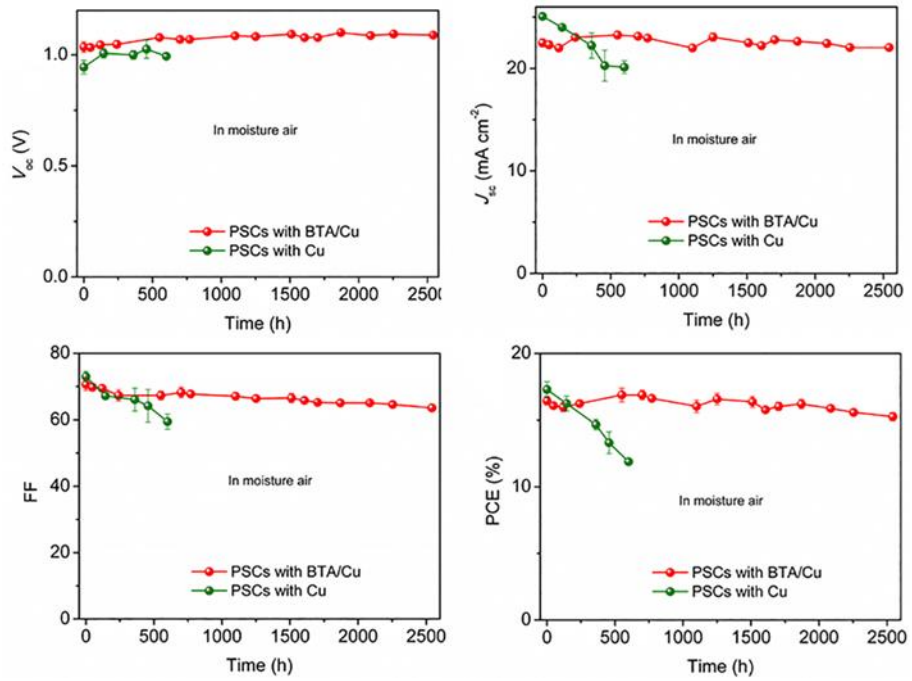

Fig. S6. Non-normalized device parameters of PSCs with BTA/Cu during aging in moisture air.

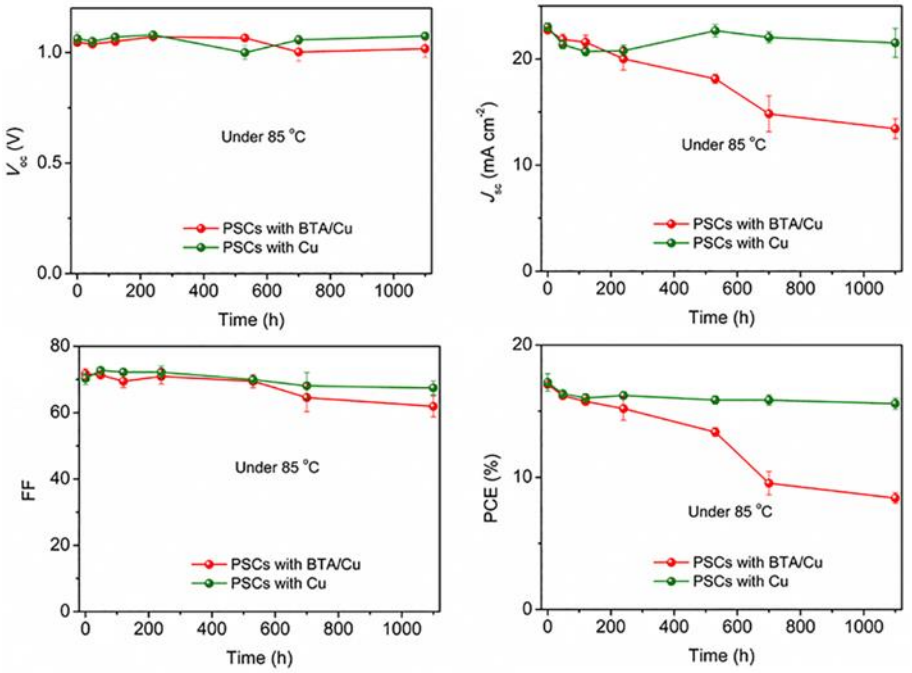

Fig. S7. Non-normalized device parameters of PSCs during aging at 85 °C.

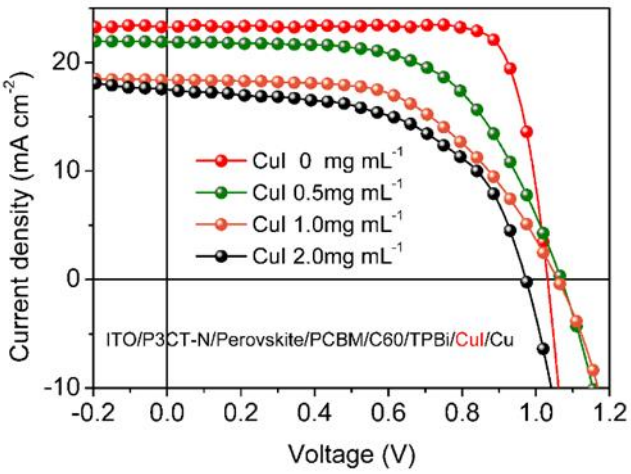

Fig. S8. *J-V* curves of PSCs through inserting CuI before Cu electrode. CuI is spin-coated using dynamic deposition process at 4000 r.p.m. for 60 s. (di-n-propyl sulfide solution).

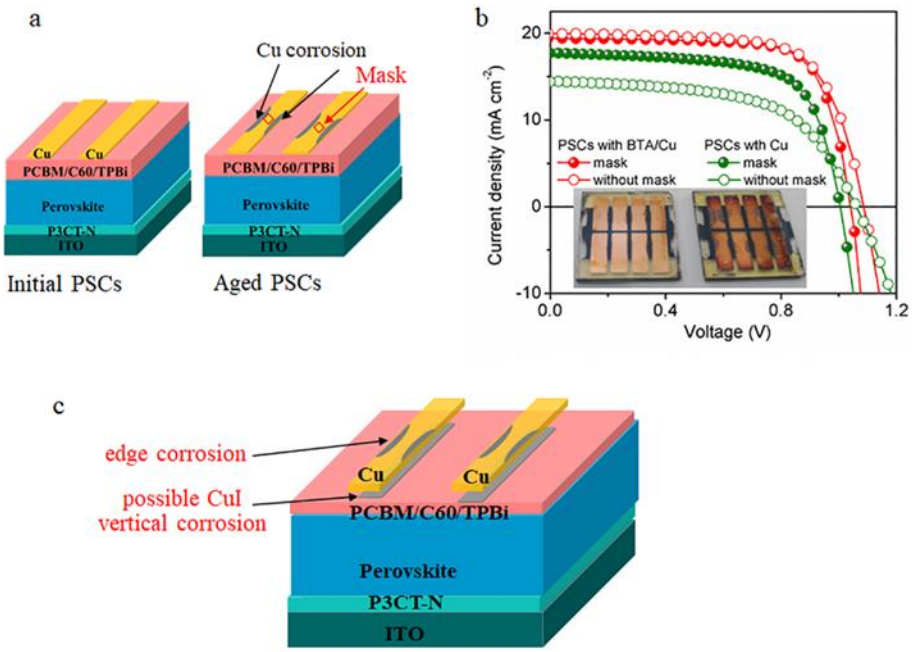

Fig. S9. Electrode corrosion induced degradation in PSCs. (a) Schematic diagram of edge corrosion in Cu electrode and the mask used to re-measure *J-V* curve in aged PSCs after aging at 85 ºC for 1100 hours. The edge corrosion of Cu electrode leads to the reducing of real device area in aged PSCs. (b) *J-V* curves of BTA/Cu based PSCs and Cu based PSCs with or without mask. Inset: photographs of aged PSCs. (c) Schematic diagram of Cu corrosion in PSCs. Photo Credit: Xiaodong Li, East China Normal University.

The most significant change is the edge corrosion of Cu electrode in control PSCs (Fig. S9b inset). Such severe edge corrosion will make the active device area in aged PSCs smaller than that in fresh PSCs (schematic diagram in Fig. S9a), which should be one reason for the J_{sc} degradation in stability test (Fig. S10 below, the major degrading parameter is J_{sc} in PSCs). To verify this point, we use a mask (4 mm^2) much smaller than device area (9 mm^2, shown in Fig. S9a) to re-measure the *I-V* curves of aged PSCs to avoid the effect of corroded edge in Cu electrode. As shown in Fig. S9b, aged PSCs with BTA/Cu exhibit similar efficiency whether with (14.91%) or without mask (15.13%). In control PSCs with Cu, the aged devices show much inferior efficiency of 8.90% without mask, mainly due to the low J_{sc} of 14.5 mA cm^{-2}. However, high J_{sc} of 17.7 mA cm^{-2} is obtained in the same device when measuring with mask, leading to superior efficiency of 12.17%. This result demonstrates that even in aged PSCs with Cu, the perovskite can still work well with moderate efficiency. That is to say, electrode corrosion induced degradation happens ahead of the degradation of perovskite layer in PSCs with Cu, which is the reason why aged devices exhibit much higher efficiency if re-measuring with mask. Apart from visible edge corrosion of Cu electrode, the reaction between Cu and perovskite can also induce vertical corrosion and maybe form CuI at Cu/PCBM interface (Fig S9c). Fig. S8 has shown that CuI inserting will lead to efficiency loss in PSCs. In addition, the reaction will also induce or accelerate the degradation of perovskite itself. Due to the two points mentioned above, even if both re-measuring with mask, the aged PSCs with Cu still exhibit obviously lower efficiency (12.17%) than PSCs with BTA/Cu (14.91%).

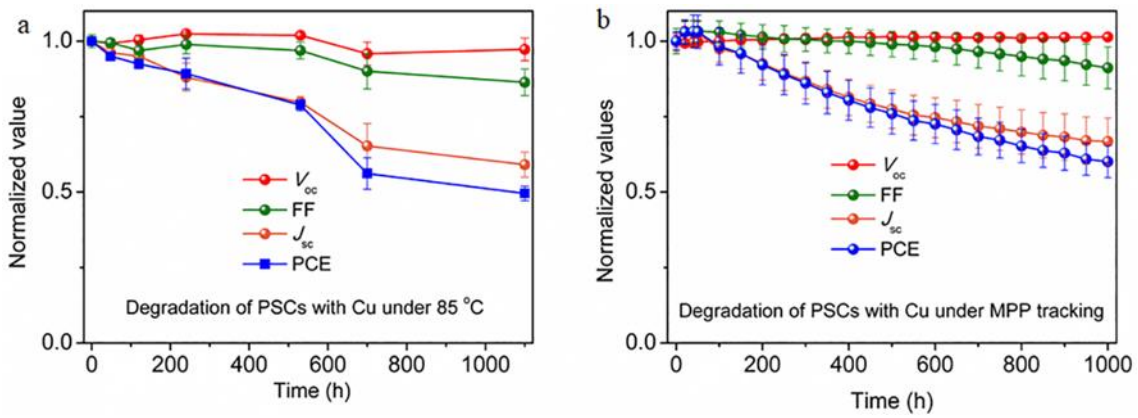

Fig. S10. Degradation analysis of V_{oc}, J_{sc}, FF and PCE of PSCs with Cu during (a) 85 ºC aging and (b) continuous MPP tracking.

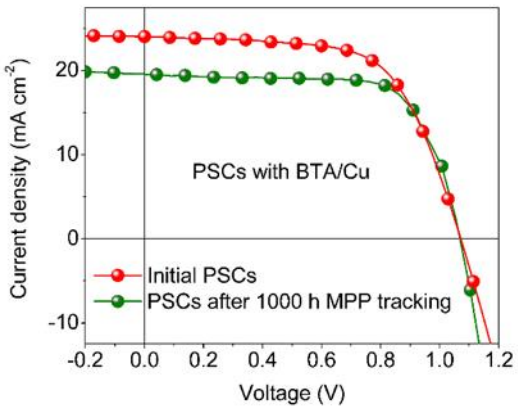

Fig. S11. *J-V* curves of PSCs with BTA/Cu before and after 1000 hours MPP tracking.

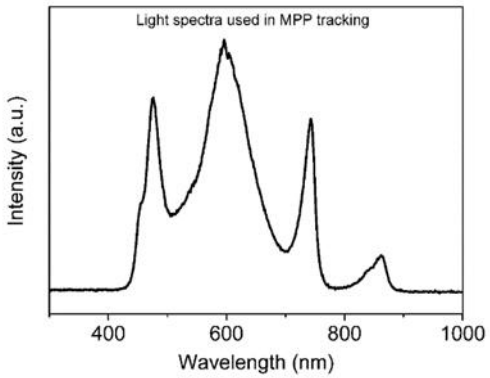

Fig. S12. Light spectra of white LED lamp used in MPP tracking.

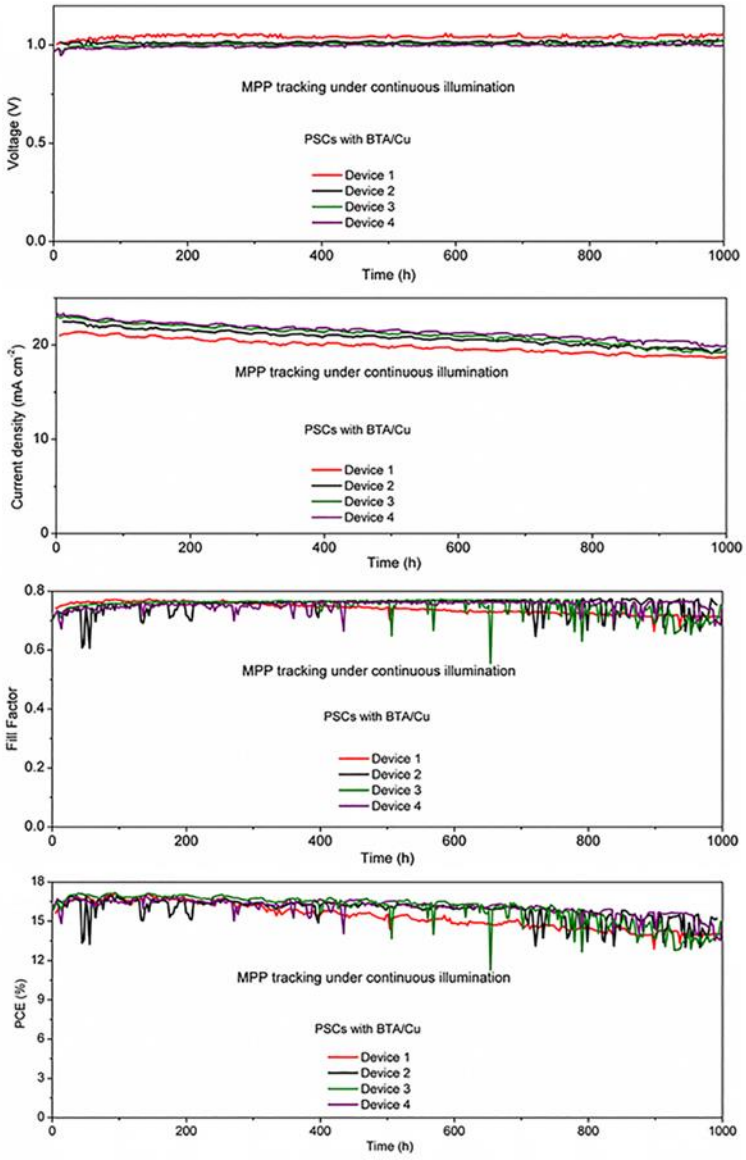

Fig. S13. Non-normalized device efficiency of PSCs with BTA/Cu during MPP tracking. Device 1, 2, 3, 4 represents the 4 devices measured in MPP tracking.

BTA concentration (mg mL^{-1})	**V_{oc} (V)**	**J_{sc} (mA cm^{-2})**	**FF (%)**	**PCE (%)**
0	1.06	24.97	76.2	20.15
0.5	1.04	24.22	79.5	19.94
1	1.10	23.17	76.4	19.56
2	1.04	22.86	75.3	17.79
5	1.02	22.11	73.5	16.40

Table S1. Photovoltaic parameters of BTA/Cu-based PSCs with different concentration of BTA.